

Measurement of Branching Fractions for $B \rightarrow \pi\pi$, $K\pi$, and KK Decays

K. Abe,¹⁰ K. Abe,³⁷ I. Adachi,¹⁰ Byoung Sup Ahn,¹⁵ H. Aihara,³⁸ M. Akatsu,²⁰ G. Alimonti,⁹ Y. Asano,⁴² T. Aso,⁴¹ V. Aulchenko,² T. Aushev,¹³ A. M. Bakich,³⁴ W. Bartel,^{6,10} S. Behari,¹⁰ P. K. Behera,⁴³ D. Beilene,² A. Bondar,² A. Bozek,¹⁶ T. E. Browder,⁹ B. C. K. Casey,⁹ P. Chang,²⁴ Y. Chao,²⁴ K. F. Chen,²⁴ B. G. Cheon,³³ S.-K. Choi,⁸ Y. Choi,³³ S. Eidelman,² Y. Enari,²⁰ R. Enomoto,^{10,11} F. Fang,⁹ H. Fujii,¹⁰ M. Fukushima,¹¹ A. Garmash,^{2,10} A. Gordon,¹⁸ K. Gotow,⁴⁴ R. Guo,²² J. Haba,¹⁰ H. Hamasaki,¹⁰ K. Hanagaki,³⁰ F. Handa,³⁷ K. Hara,²⁸ T. Hara,²⁸ N. C. Hastings,¹⁸ H. Hayashii,²¹ M. Hazumi,²⁸ E. M. Heenan,¹⁸ I. Higuchi,³⁷ T. Higuchi,³⁸ H. Hirano,⁴⁰ T. Hojo,²⁸ Y. Hoshi,³⁶ W.-S. Hou,²⁴ S.-C. Hsu,²⁴ H.-C. Huang,²⁴ Y. Igarashi,¹⁰ T. Iijima,¹⁰ H. Ikeda,¹⁰ K. Inami,²⁰ A. Ishikawa,²⁰ H. Ishino,³⁹ R. Itoh,¹⁰ G. Iwai,²⁶ H. Iwasaki,¹⁰ Y. Iwasaki,¹⁰ D. J. Jackson,²⁸ P. Jalocho,¹⁶ H. K. Jang,³² M. Jones,⁹ H. Kakuno,³⁹ J. Kaneko,³⁹ J. H. Kang,⁴⁵ J. S. Kang,¹⁵ N. Katayama,¹⁰ H. Kawai,³ H. Kawai,³⁸ T. Kawasaki,²⁶ H. Kichimi,¹⁰ D. W. Kim,³³ Heejong Kim,⁴⁵ H. J. Kim,⁴⁵ Hyunwoo Kim,¹⁵ S. K. Kim,³² K. Kinoshita,⁵ S. Kobayashi,³¹ P. Krokovny,² R. Kulasiri,⁵ S. Kumar,²⁹ A. Kuzmin,² Y.-J. Kwon,⁴⁵ J. S. Lange,⁷ M. H. Lee,¹⁰ S. H. Lee,³² D. Liventsev,¹³ R.-S. Lu,²⁴ D. Marlow,³⁰ T. Matsubara,³⁸ S. Matsumoto,⁴ T. Matsumoto,²⁰ Y. Mikami,³⁷ K. Miyabayashi,²¹ H. Miyake,²⁸ H. Miyata,²⁶ G. R. Moloney,¹⁸ S. Mori,⁴² T. Mori,⁴ A. Murakami,³¹ T. Nagamine,³⁷ Y. Nagasaka,¹⁹ T. Nakadaira,³⁸ E. Nakano,²⁷ M. Nakao,¹⁰ J. W. Nam,³³ S. Narita,³⁷ S. Nishida,¹⁷ O. Nitoh,⁴⁰ S. Noguchi,²¹ T. Nozaki,¹⁰ S. Ogawa,³⁵ T. Ohshima,²⁰ T. Okabe,²⁰ S. Okuno,¹⁴ S. L. Olsen,⁹ H. Ozaki,¹⁰ P. Pakhlov,¹³ H. Palka,¹⁶ C. S. Park,³² C. W. Park,¹⁵ H. Park,¹⁵ L. S. Peak,³⁴ M. Peters,⁹ L. E. Pilonen,⁴⁴ J. L. Rodriguez,⁹ N. Root,² M. Rozanska,¹⁶ K. Rybicki,¹⁶ J. Ryuko,²⁸ H. Sagawa,¹⁰ Y. Sakai,¹⁰ H. Sakamoto,¹⁷ M. Satapathy,⁴³ A. Satpathy,^{10,5} S. Schrenk,⁵ S. Semenov,¹³ K. Senyo,²⁰ M. E. Sevier,¹⁸ H. Shibuya,³⁵ B. Shwartz,² V. Sidorov,² J. B. Singh,²⁹ S. Stanič,⁴² A. Sugi,²⁰ A. Sugiyama,²⁰ K. Sumisawa,²⁸ T. Sumiyoshi,¹⁰ J.-I. Suzuki,¹⁰ K. Suzuki,³ S. Suzuki,²⁰ S. Y. Suzuki,¹⁰ S. K. Swain,⁹ H. Tajima,³⁸ T. Takahashi,²⁷ F. Takasaki,¹⁰ M. Takita,²⁸ K. Tamai,¹⁰ N. Tamura,²⁶ J. Tanaka,³⁸ M. Tanaka,¹⁰ G. N. Taylor,¹⁸ Y. Teramoto,²⁷ M. Tomoto,²⁰ T. Tomura,³⁸ S. N. Tovey,¹⁸ K. Trabelsi,⁹ T. Tsuboyama,¹⁰ T. Tsukamoto,¹⁰ S. Uehara,¹⁰ K. Ueno,²⁴ Y. Unno,³ S. Uno,¹⁰ Y. Ushiroda,^{17,10} Y. Usov,² S. E. Vahsen,³⁰ G. Varner,⁹ K. E. Varvell,³⁴ C. C. Wang,²⁴ C. H. Wang,²³ J. G. Wang,⁴⁴ M.-Z. Wang,²⁴ Y. Watanabe,³⁹ E. Won,³² B. D. Yabsley,¹⁰ Y. Yamada,¹⁰ M. Yamaga,³⁷ A. Yamaguchi,³⁷ H. Yamamoto,⁹ Y. Yamashita,²⁵ M. Yamauchi,¹⁰ S. Yanaka,³⁹ M. Yokoyama,³⁸ Y. Yusa,³⁷ H. Yuta,¹ C. C. Zhang,¹² J. Zhang,⁴² H. W. Zhao,¹⁰ Y. Zheng,⁹ V. Zhilich,² and D. Žontar⁴²

(Belle Collaboration)

¹Aomori University, Aomori

²Budker Institute of Nuclear Physics, Novosibirsk

³Chiba University, Chiba

⁴Chuo University, Tokyo

⁵University of Cincinnati, Cincinnati, Ohio

⁶Deutsches Elektronen-Synchrotron, Hamburg

⁷University of Frankfurt, Frankfurt

⁸Gyeongsang National University, Chinju

⁹University of Hawaii, Honolulu, Hawaii

¹⁰High Energy Accelerator Research Organization (KEK), Tsukuba

¹¹Institute for Cosmic Ray Research, University of Tokyo, Tokyo

¹²Institute of High Energy Physics, Chinese Academy of Sciences, Beijing

¹³Institute for Theoretical and Experimental Physics, Moscow

¹⁴Kanagawa University, Yokohama

¹⁵Korea University, Seoul

¹⁶H. Niewodniczanski Institute of Nuclear Physics, Krakow

¹⁷Kyoto University, Kyoto

¹⁸University of Melbourne, Victoria

¹⁹Nagasaki Institute of Applied Science, Nagasaki

²⁰Nagoya University, Nagoya

²¹Nara Women's University, Nara

²²National Kaohsiung Normal University, Kaohsiung

²³National Lien-Ho Institute of Technology, Miao Li

²⁴National Taiwan University, Taipei

²⁵Nihon Dental College, Niigata

²⁶Niigata University, Niigata

²⁷Osaka City University, Osaka²⁸Osaka University, Osaka²⁹Panjab University, Chandigarh³⁰Princeton University, Princeton, New Jersey³¹Saga University, Saga³²Seoul National University, Seoul³³Sungkyunkwan University, Suwon³⁴University of Sydney, Sydney, New South Wales³⁵Toho University, Funabashi³⁶Tohoku Gakuin University, Tagajo³⁷Tohoku University, Sendai³⁸University of Tokyo, Tokyo³⁹Tokyo Institute of Technology, Tokyo⁴⁰Tokyo University of Agriculture and Technology, Tokyo⁴¹Toyama National College of Maritime Technology, Toyama⁴²University of Tsukuba, Tsukuba⁴³Utkal University, Bhubaneswer⁴⁴Virginia Polytechnic Institute and State University, Blacksburg, Virginia⁴⁵Yonsei University, Seoul

(Received 17 April 2001; published 21 August 2001)

We report measurements of the branching fractions for $B^0 \rightarrow \pi^+ \pi^-$, $K^+ \pi^-$, $K^+ K^-$, and $K^0 \pi^0$ and $B^+ \rightarrow \pi^+ \pi^0$, $K^+ \pi^0$, $K^0 \pi^+$, and $K^+ \bar{K}^0$, based on 10.4 fb^{-1} of data collected on the $\Upsilon(4S)$ resonance with the Belle detector. We find $\mathcal{B}(B^0 \rightarrow \pi^+ \pi^-) = (0.56_{-0.20-0.05}^{+0.23+0.04}) \times 10^{-5}$, $\mathcal{B}(B^0 \rightarrow K^+ \pi^-) = (1.93_{-0.32-0.06}^{+0.34+0.15}) \times 10^{-5}$, $\mathcal{B}(B^+ \rightarrow K^+ \pi^0) = (1.63_{-0.33-0.18}^{+0.35+0.16}) \times 10^{-5}$, $\mathcal{B}(B^+ \rightarrow K^0 \pi^+) = (1.37_{-0.48-0.18}^{+0.57+0.19}) \times 10^{-5}$, and $\mathcal{B}(B^0 \rightarrow K^0 \pi^0) = (1.60_{-0.59-0.27}^{+0.72+0.25}) \times 10^{-5}$. We also set upper limits on the branching fractions for $B^+ \rightarrow \pi^+ \pi^0$, $B^0 \rightarrow K^+ K^-$, and $B^+ \rightarrow K^+ \bar{K}^0$.

DOI: 10.1103/PhysRevLett.87.101801

PACS numbers: 13.25.Hw, 14.40.Nd

The charmless hadronic B decays $B \rightarrow \pi\pi$, $K\pi$, and KK provide a rich sample to test the standard model and to probe new physics [1]. Of particular interest are indirect and direct CP violation in the $\pi\pi$ and $K\pi$ modes, which are related to the angles ϕ_2 and ϕ_3 of the unitarity triangle, respectively [1]. Measurements of branching fractions of these decay modes are an important first step toward these CP violation studies. However, the only published measurements come from one experiment [2]. One of the key experimental issues is the particle identification (PID) for separation of the high momentum charged π and K mesons. This is one of the primary reasons that the B factory experiments [3,4] have been equipped with specialized high momentum PID devices.

In this paper, we report the first results of the Belle experiment on charmless hadronic two-body B decays into $\pi\pi$, $K\pi$, and KK final states. The decay modes studied are $\pi^+ \pi^-$, $K^+ \pi^-$, $K^+ K^-$, and $K^0 \pi^0$ for B^0 decays, and $\pi^+ \pi^0$, $K^+ \pi^0$, $K^0 \pi^+$, $K^+ \bar{K}^0$, for B^+ decays. For the modes with K^0 mesons, only $K_S^0 \rightarrow \pi^+ \pi^-$ decays are used. Throughout this paper, the inclusion of charge conjugate states is implied. The results are based on data taken by the Belle detector [5] at the KEKB asymmetric $e^+ e^-$ storage ring [6]. The Belle detector is equipped with aerogel Čerenkov counters (ACC) configured for high momentum PID. The data set consists of 10.4 fb^{-1} data taken at the $\Upsilon(4S)$ resonance, corresponding to $11.1 \times 10^6 B\bar{B}$ events, and 0.6 fb^{-1} data taken at an energy $\sim 60 \text{ MeV}$ be-

low the resonance, for systematic studies of the continuum $q\bar{q}$ background.

Primary charged tracks are required to satisfy track quality cuts based on their impact parameters relative to the interaction point (IP). K_S^0 mesons are reconstructed using pairs of charged tracks that have an invariant mass within $\pm 30 \text{ MeV}/c^2$ of the known K_S^0 mass and a well reconstructed vertex that is displaced from the IP. Candidate π^0 mesons are reconstructed using γ pairs with an invariant mass within $\pm 16 \text{ MeV}/c^2$ of the nominal π^0 mass. The B meson candidates are reconstructed using the beam constrained mass, $m_{bc} = \sqrt{E_{\text{beam}}^2 - p_B^2}$, and the energy difference, $\Delta E = E_B - E_{\text{beam}}$, where $E_{\text{beam}} \equiv \sqrt{s}/2 \simeq 5.290 \text{ GeV}$, and p_B and E_B are the momentum and energy of the reconstructed B in the $\Upsilon(4S)$ rest frame, respectively. The signal region for each variable is defined as $\pm 3\sigma$ from its central value. The resolution in m_{bc} is dominated by the beam energy spread and is typically $2.7 \text{ MeV}/c^2$. The ΔE resolution ranges from 20 to 25 MeV, depending on the momentum and energy resolutions for each particle. Unless otherwise stated, we compute ΔE assuming a π mass for each charged particle. This shifts ΔE downward by 44 MeV for each charged K meson, giving kinematic separation between the $h\pi^+$ and hK^+ ($h = \pi, K$) final states. In modes with π^0 mesons, both the m_{bc} and ΔE distributions are asymmetric due to γ interactions in the material in front of the calorimeter and energy leakage out of the calorimeter.

We accept events in the region $m_{bc} > 5.2 \text{ GeV}/c^2$ and $|\Delta E| < 0.25 \text{ GeV}$ for the h^+h^- and $K_S^0 h^+$ modes, and $-0.45 < \Delta E < 0.15 \text{ GeV}$ for the $h^+\pi^0$ and $K_S^0\pi^0$ modes. In this kinematic window, the area outside the signal region is defined as a sideband. The signal reconstruction efficiencies after the kinematic window cut are 65% for h^+h^- , 33% for $K_S^0 h^+$, 50% for $h^+\pi^0$, and 24% for $K_S^0\pi^0$, according to a GEANT [7] based Monte Carlo (MC) simulation. The MC tracking efficiency is verified by detailed studies using high momentum tracks from D , η , and K^* decays. The reconstruction efficiencies for high momentum K_S^0 and π^0 mesons are tested by comparing the ratio of the yield of $D^+ \rightarrow K_S^0\pi^+$ to $D^+ \rightarrow K^-\pi^+\pi^+$ and $D^0 \rightarrow K^-\pi^+\pi^0$ to $D^0 \rightarrow K^-\pi^+$, respectively, between data and MC simulation. From these studies, we assign a relative systematic error in these efficiencies of 2.3% per charged track, 12% per K_S^0 , and 8.5% per π^0 meson.

The background from $b \rightarrow c$ transitions is negligible. The dominant background is from the continuum $q\bar{q}$ process. We suppress this background using the event topology, which is spherical for $B\bar{B}$ events and jetlike for $q\bar{q}$ events in the $Y(4S)$ rest frame. This difference can be quantified by using several variables including the event sphericity, S , the angle between the B candidate thrust axis and the thrust axis of the rest of the event, θ_T , and the Fox-Wolfram moments [8] $H_l = \sum_{i,j} |\vec{p}_i| |\vec{p}_j| P_l(\cos\theta_{ij})$, where the indices i and j run over all final state particles, \vec{p}_i and \vec{p}_j are the momentum vectors of particles i and j , P_l is the l th Legendre polynomial, and θ_{ij} is the angle between particles i and j . We can also use the B flight direction, θ_B , and the decay axis direction, θ_{hh} , which distinguish $B\bar{B}$ from $q\bar{q}$ processes based on initial state angular momentum.

We increase the suppression power of the normalized Fox-Wolfram moments, $R_l = H_l/H_0$, by decomposing them into three terms: $R_l = R_l^{ss} + R_l^{so} + R_l^{oo} = (H_l^{ss} + H_l^{so} + H_l^{oo})/H_0$, where the indices ss , so , and oo indicate, respectively, that both, one, or neither of the particles comes from a B candidate. These are combined into a six term Fisher discriminant [9] called the super-Fox-Wolfram [10] defined as $\text{SFW} = \sum_{l=1}^4 (\alpha_l R_l^{so} + \beta_l R_l^{oo})$, where α_l and β_l are Fisher coefficients and $l = 2, 4$ for α_l and R_l^{so} . The terms R_l^{ss} and $R_{l=1,3}^{so}$ are excluded because they are strongly correlated with m_{bc} and ΔE . In the h^+h^- modes, for example, SFW gives a 20% increase in the expected significance compared to R_2 .

We combine different $q\bar{q}$ suppression variables into a single likelihood, $\mathcal{L}_{s(q\bar{q})} = \prod_i \mathcal{L}_s^i(q\bar{q})$, where the $\mathcal{L}_s^i(q\bar{q})$ denotes the signal ($q\bar{q}$) likelihood of the suppression variable i , and select candidate events by cutting on the likelihood ratio $\mathcal{R}_s = \mathcal{L}_s/(\mathcal{L}_s + \mathcal{L}_{q\bar{q}})$. For h^+h^- and $K_S^0 h^+$, the likelihood contains SFW, $\cos\theta_B$, and $\cos\theta_{hh}$. In modes with π^0 mesons, the $q\bar{q}$ background is significantly larger.

In this case, we first make a loose cut on $\cos\theta_T$. Next, we extend SFW to include $\cos\theta_T$ and S , and form the likelihood using this extended SFW and $\cos\theta_B$. In each case, the signal probability density functions (PDFs) are determined using MC simulation and the $q\bar{q}$ PDFs are taken from m_{bc} sideband data. The performance of \mathcal{R}_s varies among the modes with efficiencies ranging from 40% to 51% while removing more than 95% of the $q\bar{q}$ background. The $\pi^+\pi^0$ mode calls for a tighter cut with an efficiency of 26%. The error in these efficiencies is determined by applying the same procedure to the $B^+ \rightarrow \bar{D}^0\pi^+$, $\bar{D}^0 \rightarrow K^-\pi^+$ event sample and comparing the cut efficiencies between data and MC. The relative systematic error is determined to be 4%.

The high momentum charged π and K mesons ($1.5 < p_{h^\pm} < 4.5 \text{ GeV}/c$ in the laboratory frame) are distinguished by cutting on the $\pi(K)$ likelihood ratio $\mathcal{R}_{\pi(K)} \equiv \mathcal{L}_{\pi(K)}/(\mathcal{L}_\pi + \mathcal{L}_K)$, where $\mathcal{L}_{\pi(K)}$ denotes the product of each $\pi(K)$ likelihood of their energy loss (dE/dx) in the central drift chamber and their Čerenkov light yield in the ACC. Each likelihood is calculated from a PDF determined using MC simulation. The PID efficiency and fake rate are measured using π and K tracks in the same kinematic range as signal, with kinematically selected $D^{*+} \rightarrow D^0\pi^+$, $D^0 \rightarrow K^-\pi^+$ decays. The efficiency and fake rate for π mesons are measured to be 92% and 4% (true π fakes K), whereas those for K mesons are 85% and 10% (true K fakes π), respectively. The relative systematic error in the PID efficiency is 2.5% per charged π or K meson.

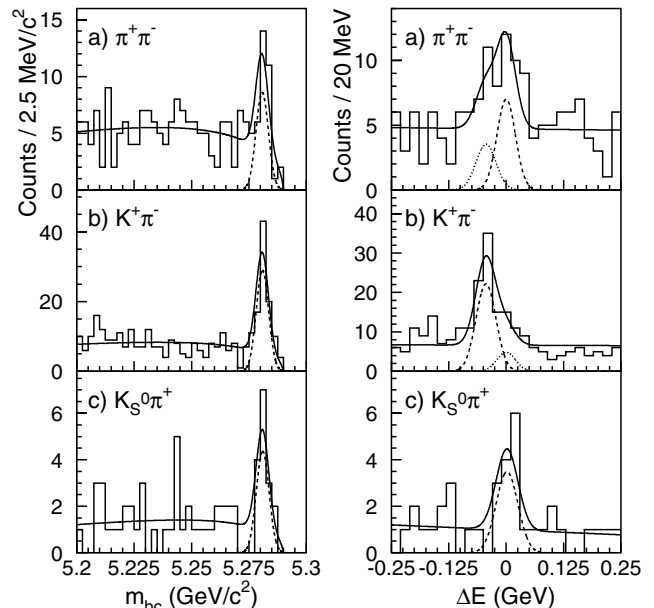


FIG. 1. The m_{bc} (left) and ΔE (right) distributions, in the signal region of the other variable, for $B \rightarrow$ (a) $\pi^+\pi^-$, (b) $K^+\pi^-$, and (c) $K_S^0\pi^+$. The fit function and its signal component are shown by the solid and dashed curve, respectively. In the $\pi^+\pi^-$ and $K^+\pi^-$ fits, the cross-talk components are shown by dotted curves.

TABLE I. Summary of the results. The obtained signal yield (N_s), statistical significance (Σ), efficiency (ϵ), charge averaged branching fraction (\mathcal{B}), and its 90% confidence level upper limit (U.L.) are shown. In the calculation of \mathcal{B} , the production rates of B^+B^- and $B^0\bar{B}^0$ pairs are assumed to be equal. In the modes with K^0 mesons, N_s and ϵ are quoted for K_S^0 , while \mathcal{B} and U.L. are for K^0 . Submode branching fractions for $K_S^0 \rightarrow \pi^+\pi^-$ and $\pi^0 \rightarrow \gamma\gamma$ are included in ϵ . The first and second errors in N_s and \mathcal{B} are statistical and systematic errors, respectively.

Mode	N_s	Σ	ϵ (%)	\mathcal{B} ($\times 10^{-5}$)	U.L. ($\times 10^{-5}$)
$B^0 \rightarrow \pi^+\pi^-$	$17.7^{+7.1+0.3}_{-6.4-1.1}$	3.1	28.1	$0.56^{+0.23+0.04}_{-0.20-0.05}$...
$B^+ \rightarrow \pi^+\pi^0$	$10.4^{+5.1+1.2}_{-4.3-1.6}$	2.7	12.0	$0.78^{+0.38+0.08}_{-0.32-0.12}$	1.34
$B^0 \rightarrow K^+\pi^-$	$60.3^{+10.6+2.7}_{-9.9-1.1}$	7.8	28.0	$1.93^{+0.34+0.15}_{-0.32-0.06}$...
$B^+ \rightarrow K^+\pi^0$	$34.9^{+7.6+0.6}_{-7.0-2.0}$	7.2	19.2	$1.63^{+0.35+0.16}_{-0.33-0.18}$...
$B^+ \rightarrow K^0\pi^+$	$10.3^{+4.3+0.4}_{-3.6-0.1}$	3.5	13.5	$1.37^{+0.57+0.19}_{-0.48-0.18}$...
$B^0 \rightarrow K^0\pi^0$	$8.4^{+3.8+0.4}_{-3.1-0.6}$	3.9	9.4	$1.60^{+0.72+0.25}_{-0.59-0.27}$...
$B^0 \rightarrow K^+K^-$	$0.2^{+3.8}_{-0.2}$...	24.0	...	0.27
$B^+ \rightarrow K^+\bar{K}^0$	$0.0^{+0.9}_{-0.0}$...	12.1	...	0.50

Figure 1 shows the m_{bc} and ΔE distributions in the signal region of the other variable, for the $\pi^+\pi^-$, $K^+\pi^-$, and $K_S^0\pi^+$ modes. Each m_{bc} and ΔE distribution is fitted to a Gaussian signal plus a background function. The m_{bc} and ΔE peak positions and m_{bc} width are calibrated using the $B^+ \rightarrow \bar{D}^0\pi^+$, $\bar{D}^0 \rightarrow K^+\pi^-$ data sample. The ΔE Gaussian width is calibrated using high momentum $D^0 \rightarrow K^-\pi^+$ and $D^+ \rightarrow K_S^0\pi^+$ decays. The m_{bc} background shape is modeled by the ARGUS background function [11] with parameters determined using positive ΔE sideband data. A linear function is used to model the shape of the ΔE background; the slope is fixed at the value determined from the m_{bc} sideband. The signal yields are determined from the ΔE fits where there is kinematic separation between the $h\pi^+$ and hK^+ decays. The $\pi^+\pi^-$ and $K^+\pi^-$ fits include a component to account for misidentified backgrounds. The normalizations of these components are free parameters. The extracted yields are listed in Table I. The cross talk among different signal modes is consistent with expectations based on PID fake rates. For the K^+K^- and $K^+K_S^0$ modes, the yields obtained from the fit are less than one event.

Figure 2 shows the m_{bc} and ΔE projections for the $\pi^+\pi^0$, $K^+\pi^0$, and $K_S^0\pi^0$ modes. For these modes, since the ΔE distribution has a long tail, a two-dimensional fit is applied to the m_{bc} and ΔE distributions. The signal distribution is modeled by a smoothed two-dimensional MC histogram, while the background distribution is taken to be the product of the m_{bc} and ΔE background functions discussed above. The signal and background shapes are determined following the same procedure as for the h^+h^- and $K_S^0h^+$ modes. The ΔE resolution is calibrated using $D^0 \rightarrow K^-\pi^+\pi^0$ decays where the π^0 is reconstructed in the same kinematic range as the signal. For the $\pi^+\pi^0$ mode, since the cross talk from $K^+\pi^0$ is expected to be large and the ΔE separation is less than 1σ , the $K^+\pi^0$ component is fixed at its expected level. The obtained yields are listed in Table I.

The systematic error in the signal yield is determined by varying the parameters of the fitting functions within $\pm 1\sigma$ of their nominal values. The changes in the signal yield from each variation are added in quadrature. These errors range from 1% to 6%. In the $K^+\pi^-$ mode, the ΔE background normalization is influenced by an excess around -175 MeV. In this region, we expect to observe a few background events from B decays such as $B \rightarrow \rho\pi$, $K^*\pi$, and $K^*\gamma$ (for modes with π^0 mesons), based on a MC simulation [12,13] in all signal modes. To estimate

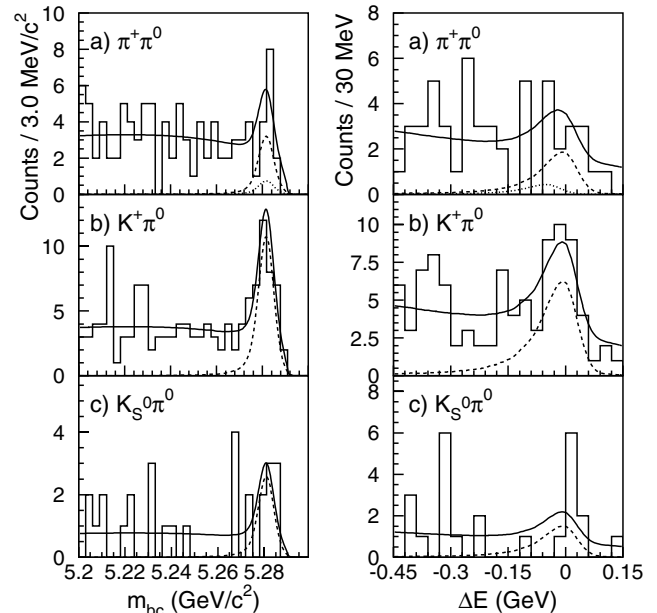


FIG. 2. The m_{bc} (left) and ΔE (right) projections for $B \rightarrow$ (a) $\pi^+\pi^0$, (b) $K^+\pi^0$, and (c) $K_S^0\pi^0$. For $K^+\pi^0$, a K mass is assumed for the charged particle. The projection of the two-dimensional fit onto each variable and its signal component are shown by the solid and dashed curves, respectively. In the $\pi^+\pi^0$ fit, the cross talk from $K^+\pi^0$ is indicated by a dotted curve.

TABLE II. Ratio of charge averaged branching fractions (\mathcal{B}) for $B \rightarrow \pi\pi$ and $K\pi$ decays. The first error is statistical and the second is systematic. The correlation and cancellation of systematic errors are taken into account. A 90% confidence level upper limit in the first ratio is calculated using a similar method as the upper limit of \mathcal{B} described in text.

Modes	Ratio
$\mathcal{B}(B^+ \rightarrow \pi^+ \pi^0)/\mathcal{B}(B^0 \rightarrow \pi^+ \pi^-)$	<2.67
$2\mathcal{B}(B^+ \rightarrow K^+ \pi^0)/\mathcal{B}(B^0 \rightarrow K^+ \pi^-)$	$1.69^{+0.46+0.17}_{-0.45-0.19}$
$\mathcal{B}(B^0 \rightarrow \pi^+ \pi^-)/\mathcal{B}(B^0 \rightarrow K^+ \pi^-)$	$0.29^{+0.13+0.01}_{-0.12-0.02}$
$\mathcal{B}(B^0 \rightarrow K^+ \pi^-)/2\mathcal{B}(B^0 \rightarrow K^0 \pi^0)$	$0.60^{+0.25+0.11}_{-0.29-0.16}$
$2\mathcal{B}(B^+ \rightarrow K^+ \pi^0)/\mathcal{B}(B^+ \rightarrow K^0 \pi^+)$	$2.38^{+0.98+0.39}_{-1.10-0.26}$
$\mathcal{B}(B^0 \rightarrow K^+ \pi^-)/\mathcal{B}(B^+ \rightarrow K^0 \pi^+)$	$1.41^{+0.55+0.22}_{-0.63-0.20}$

their effect, we either exclude the negative ΔE sideband from the fit or add these components to the fit based on MC histograms. The resulting change in the signal yield, ranging from 4% to 10%, is added in quadrature to the above systematic error.

Table I summarizes all results. The statistical significance (Σ) is defined as $\sqrt{-2 \ln[\mathcal{L}(0)/\mathcal{L}_{\max}]}$, where \mathcal{L}_{\max} and $\mathcal{L}(0)$ denote the maximum likelihood with the nominal signal yield and with the signal yield fixed at zero, respectively [12]. The final systematic error is the quadratic sum of the relative error in the signal yield (N_s), the reconstruction, PID, and continuum suppression efficiencies, and the number of $B\bar{B}$ pairs (1%). If $\Sigma < 3$, we set a 90% confidence level upper limit on the signal yield ($N_s^{\text{U.L.}}$) from the relation $\int_0^{N_s^{\text{U.L.}}} \mathcal{L}(N_s) dN_s / \int_0^\infty \mathcal{L}(N_s) dN_s = 0.9$, where $\mathcal{L}(N_s)$ denotes the maximum likelihood with the signal yield fixed at N_s . The branching fraction upper limit (U.L.) is then calculated by increasing $N_s^{\text{U.L.}}$ and reducing the efficiency by their systematic errors.

In summary, using 11.1×10^6 $B\bar{B}$ events recorded in the Belle detector, the charge averaged branching fractions for $B \rightarrow \pi^+ \pi^-$, $K^+ \pi^-$, $K^+ \pi^0$, $K^0 \pi^+$, and $K^0 \pi^0$ are measured with statistically significant signals. For the $\pi^+ \pi^0$ mode, an excess is seen with marginal significance. No excess is observed for the $K^+ K^-$ and $K^+ \bar{K}^0$ modes. For these modes, 90% confidence level upper limits are set. The results are listed in Table I. In Table II, we list some ratios of branching fractions based on these measurements. Recent theoretical work [1] suggests that the ratio $\mathcal{B}(B^+ \rightarrow \pi^+ \pi^0)/\mathcal{B}(B^0 \rightarrow \pi^+ \pi^-)$ is relevant for extracting ϕ_2 , the ratio $\mathcal{B}(B^+ \rightarrow K^+ \pi^0)/\mathcal{B}(B^0 \rightarrow K^+ \pi^-)$ is relevant for determining the contribution from electroweak penguins, and the remaining four ratios are useful to constrain ϕ_3 . All the branching fraction and ratio results are consistent with other measurements [2,4]. Our results confirm that $\mathcal{B}(B^0 \rightarrow K^+ \pi^-)$ is larger than $\mathcal{B}(B^0 \rightarrow \pi^+ \pi^-)$, and indicate that $\mathcal{B}(B^+ \rightarrow h^+ \pi^0)$ and $\mathcal{B}(B^0 \rightarrow K^0 \pi^0)$ seem

to be larger than expected in relation to the $B^0 \rightarrow h^+ \pi^-$ and $B^+ \rightarrow K^0 \pi^+$ modes based on isospin or penguin dominance arguments [1].

We thank the KEKB accelerator group for the excellent operation of the KEKB accelerator. We acknowledge support from the Ministry of Education, Culture, Sports, Science, and Technology of Japan and the Japan Society for the Promotion of Science; the Australian Research Council and the Australian Department of Industry, Science and Resources; the Department of Science and Technology of India; the BK21 program of the Ministry of Education of Korea and the CHEP SRC program of the Korea Science and Engineering Foundation; the Polish State Committee for Scientific Research under Contract No. 2P03B 17017; the Ministry of Science and Technology of Russian Federation; the National Science Council and the Ministry of Education of Taiwan; the Japan-Taiwan Cooperative Program of the Interchange Association; and the U.S. Department of Energy.

- [1] For theory discussions, see, for example, A. J. Buras and R. Fleischer, *Eur. Phys. J. C* **16**, 97 (2000); M. Beneke, G. Buchalla, M. Neubert, and C. T. Sachrajda, *Nucl. Phys. B* **591**, 313 (2000); J. Rosner, in *Lecture Notes TASI-2000* (World Scientific, Singapore, 2001); Y. Y. Keum, H. N. Li, and A. I. Sanda, *Phys. Rev. D* **63**, 054008 (2001).
- [2] CLEO Collaboration, D. Cronin-Hennessy *et al.*, *Phys. Rev. Lett.* **85**, 515 (2000).
- [3] Belle Collaboration, P. Chang *et al.*, in *Proceedings of the 30th International Conference on High Energy Physics (ICHEP)*, edited by C. S. Lim and T. Yamanaka (World Scientific, Singapore, 2001).
- [4] BABAR Collaboration, T. Champion *et al.*, in *Proceedings of the 30th International Conference on High Energy Physics (ICHEP)* (Ref. [3]).
- [5] Belle Collaboration, K. Abe *et al.*, KEK Progress Report No. 2000-4, 2000 [Nucl. Instrum. Methods Phys. Res., Sect. A. (to be published)].
- [6] KEKB B Factory Design Report, KEK Report No. 95-7, 1995 (unpublished).
- [7] R. Brun *et al.*, GEANT 3.21, CERN Report No. DD/EE/84-1, 1987.
- [8] G. Fox and S. Wolfram, *Phys. Rev. Lett.* **41**, 1581 (1978).
- [9] R. A. Fisher, *Ann. Eugenics* **7**, 179 (1936).
- [10] The super-Fox-Wolfram was first proposed as an extension of R_2 in a series of lectures on continuum suppression at KEK by R. Enomoto in 1999.
- [11] H. Albrecht *et al.*, *Phys. Lett. B* **241**, 278 (1990).
- [12] Particle Data Group, D. E. Groom *et al.*, *Eur. Phys. J. C* **15**, 1 (2000).
- [13] CLEO Collaboration, D. Cinabro *et al.*, in *Proceedings of the 30th International Conference on High Energy Physics (ICHEP)* (Ref. [3]); CLEO Collaboration, R. Stroynowski *et al.*, *ibid.*